Ras activation and symmetry breaking during Dictyostelium chemotaxis

Kortholt, Arjan; Keizer-Gunnink, Ineke; Kataria, Rama; Van Haastert, Peter J. M.

Published in:
Journal of Cell Science

DOI:
10.1242/jcs.132340

Publication date:
2013

Ras activation and symmetry breaking during *Dictyostelium* chemotaxis

Arjan Kortholt, Ineke Keizer-Gunnink, Rama Kataria and Peter J. M. Van Haastert*

Department of Cell Biochemistry, University of Groningen, Nijenborgh 7, 9747 AG Groningen, The Netherlands

*Author for correspondence (P.J.M.van.haastert@rug.nl)

Accepted 9 July 2013
Journal of Cell Science 126, 4502–4513

doi: 10.1242/jcs.132340

Summary

Central to chemotaxis is the molecular mechanism by which a shallow spatial gradient of chemoattractant induces symmetry breaking of activated signaling molecules. Previously, we have used *Dictyostelium* mutants to investigate the minimal requirements for chemotaxis, and identified a basal signaling module providing activation of Ras and F-actin at the leading edge. Here, we show that Ras activation after application of a pipette releasing the chemoattractant cAMP has three phases, each depending on specific guanine-nucleotide-exchange factors (GEFs). Initially a transient activation of Ras occurs at the entire cell boundary, which is proportional to the local cAMP concentrations and therefore slightly stronger at the front than in the rear of the cell. This transient Ras activation is present in *gα2* (*gpbB*)-null cells but not in *gβ* (*gpbA*)-null cells, suggesting that Gβγ mediates the initial activation of Ras. The second phase is symmetry breaking: Ras is activated only at the side of the cell closest to the pipette. Symmetry breaking absolutely requires Gα2 and Gβγ, but not the cytoskeleton or four cAMP-induced signaling pathways, those dependent on phosphatidylinositol (3,4,5)-triphosphate [PtdIns(3,4,5)P_3], cGMP, TorC2 and PLA2. As cells move in the gradient, the crescent of activated Ras in the front half of the cell becomes confined to a small area at the utmost front of the cell. Confinement of Ras activation leads to cell polarization, and depends on cGMP formation, myosin and F-actin. The experiments show that activation, symmetry breaking and confinement of Ras during *Dictyostelium* chemotaxis uses different G-protein subunits and a multitude of Ras GEFs and GTPase-activating proteins (GAPs).

Key words: Chemotaxis, Shallow gradients, Ras, Amplification, Synergy, Symmetry breaking

Introduction

Ras belongs to the family of small G-proteins that function as molecular switches to control a wide variety of important cellular functions. They switch between an inactive GDP-bound and active GTP-bound state. Ras activity is regulated by guanine-nucleotide-exchange factors (GEFs) that catalyze the exchange of GDP for GTP, thereby activating the Ras protein. GTPase-activating proteins (GAPs) stimulate an otherwise low intrinsic GTPase activity by many orders of magnitude, thereby converting the protein back into the inactive GDP-bound form (Bourne et al., 1991; Vetter and Wittinghofer, 2001).

Owing to its genetic tractability and high conservation of many important signaling pathways, *Dictyostelium* has proven to be an excellent model for studying small G-protein signaling (Charest and Firtel, 2007; Kortholt and van Haastert, 2008; Rivero and Somesh, 2002; Sasaki et al., 2004; Weeks, 2005). Genetic studies have shown that Ras proteins are involved in regulation of the cytoskeleton, cell cycle, growth, cell polarity, chemotaxis, and photo- and thermotaxis of multicellular slugs (Chubb et al., 2000; Chubb et al., 2002; Reymond et al., 1984; Sutherland et al., 2001; Weeks, 2005; Wilkins et al., 2000b). RasC and RasG are the best-characterized *Dictyostelium* Ras proteins; both are activated in response to cAMP (Kae et al., 2004), and are important for the regulation of the cAMP relay and cAMP-mediated chemotaxis, respectively (Bolourani et al., 2006; Charest et al., 2010; Lim et al., 2001; Lim et al., 2005; Tuxworth et al., 1997).

Gradients of diffusive chemicals give rise to chemotaxis (Hoeller and Kay, 2007; Swaney et al., 2010). Sensitive cells, such as *Dictyostelium* or neutrophils, can detect very shallow spatial gradients of ~1% concentration difference across the cell (Mato et al., 1975). Concepts from physics and mathematical models have been employed to understand how cells can detect such minute spatial signals against a large background of mean chemoattractant concentration. These concepts include symmetry breaking to generate a front and rear, signal amplification to enhance spatial differences and time averaging of spatial information to reduce stochastic noise (Ambrosi et al., 2004; Causin and Facchetti, 2009; Tranquillo et al., 1988; Ueda and Shibata, 2007; van Haastert and Postma, 2007).

The signal transduction cascade for chemotaxis consists of surface receptors, heterotrimeric and small G-proteins, and numerous signaling enzymes, leading to the local activation of the cytoskeleton, predominantly F-actin at the front, and myosin filaments at the side and the rear of the cell. In *Dictyostelium*, a shallow gradient of cAMP induces the activation of cAMP receptors and the associated heterotrimeric G-protein Gα2βγ in a manner that is approximately proportional to the steepness of the gradient (Elzie et al., 2009; Jin et al., 2000; Xiao et al., 1997). In contrast, activation of Ras is much stronger in the front than in the rear of chemotaxing cells (Charest et al., 2010; Kortholt et al., 2011; Sasaki et al., 2004; Sasaki and Firtel, 2006; Zhang et al., 2008). Several studies have shown that inactivation of both *rasC* and *rasG* results in defective cAMP-mediated chemotaxis (Bolourani et al., 2006; Kortholt et al., 2011). Four signaling enzymes, PI3K, TorC2, PLA2 and sGC, have been implicated in chemotaxis (Chen et al., 2007; Kamimura et al., 2008; Liao et al.,

2010; Veltman et al., 2008). Cells lacking all four enzyme activities show normal Ras activation in cAMP gradients, but can only exhibit chemotaxis in steep cAMP gradients (Kortholt et al., 2011). These observations suggest that symmetry breaking during chemotaxis occurs at the level of Ras activation, and that activation of downstream signaling pathways is not essential for Ras activation and chemotaxis.

Dictyostelium Ras activation occurs downstream of heterotrimeric G-protein signaling (Kae et al., 2004; Sasaki et al., 2004), but the exact mechanism is not well understood. Here we used a sensitive assay to visualize Ras activation in cells in defined gradients of cAMP. We show that Ras activation after application of a stable cAMP gradient has three phases. Initially, a transient activation of Ras occurs at the entire cell boundary, which is proportional to the local cAMP concentrations and therefore slightly stronger at the front than in the rear of the cell. The second phase is symmetry breaking: Ras is activated only at the side of the cell closest to the pipette. During the third phase, the crescent of activated Ras in the front half of the cell becomes confined to a small area at the utmost front of the cell. Mutant studies revealed that activation, symmetry breaking and confinement during *Dictyostelium* chemotaxis use different G-protein subunits and a multitude of Ras GEFs and GAPs. Taken together, these experiments provide a conceptual framework to explain the exquisite sensitivity of cells in sensing shallow gradients of chemoattractants.

Results

A sensitive assay for Ras activation at the cell boundary

Ras proteins are localized approximately uniformly at the plasma membrane of *Dictyostelium* cells (Sasaki et al., 2004; Sasaki and Firtel, 2009). Stimulation of cells with cAMP does not change the localization of Ras, but locally stimulates the conversion of Ras from the inactive Ras-GDP state to active Ras-GTP (Sasaki et al., 2004; Sasaki and Firtel, 2009). The RBD domain of mammalian Raf binds specifically to the GTP-bound form of Ras. Ras activation can therefore be observed by monitoring the translocation of RBD-Raf–GFP from the cytoplasm to the cell boundary (Kortholt et al., 2011; Sasaki et al., 2004; Sasaki and Firtel, 2009). Because boundary pixels also contain cytoplasm, translocation assays are fundamentally insensitive (Bosgraaf et al., 2008). Here, we used a more sensitive assay to detect Ras-GTP by co-expressing cytosolic RFP with RBD-Raf–GFP. In each boundary pixel (i) the fluorescence intensity of cytosolic RFP (cR_i) refers to the volume of cytosol in that pixel (see Materials and Methods). The fluorescence intensity of RBD-Raf–GFP specifically bound to Ras-GTP at the membrane in that pixel (Ψ) is the total GFP fluorescence intensity (G_i) minus the fluorescence intensity of RFP. For direct comparison among different cells and strains, data are presented as the level of RBD-Raf–GFP at the cell membrane relative to the average level of RBD-Raf–GFP in the cytosol (G_{cyt}), $\Psi=(G_i-cR_i)/<G_{cyt}>$.

Cells in buffer exhibit intrinsic symmetry breaking of active Ras

In buffer, RBD-Raf–GFP seems to be localized approximately uniformly in the cell, with little detectable enhanced localization at the boundary. However, after subtraction of RBD-Raf–GFP in the cytoplasm using cytosolic RFP, it appears that boundary pixels retain a significant amount of RBD-Raf–GFP (Fig. 1A; supplementary material Movie 1). RBD-Raf–GFP is clearly present at the cell membrane in the extending pseudopods, but is also detectable at the plasma membrane of other parts of the cell (Fig. 1A). RBD-Raf–GFP at the membrane (Ψ) was measured around the circumference of 14 cells (Fig. 1B). The front of the cell is defined by the center boundary point of the extending pseudopod; RBD-Raf–GFP at the membrane in this point is $\Psi=0.53\pm0.07$ (i.e. RBD-Raf–GFP at the membrane is $53\pm7\%$ that of RBD-Raf–GFP the cytoplasm; mean±s.d., $n=14$ cells). The membrane at the rear of the cell contains RBD-Raf–GFP at a level of $\Psi=0.10\pm0.05$, approximately a fifth that in the pseudopod. The experiments demonstrate that cells in buffer exhibit intrinsic symmetry breaking of activated Ras. The front half of the cell contains ~3-fold more activated Ras than the rear-half of the cell.

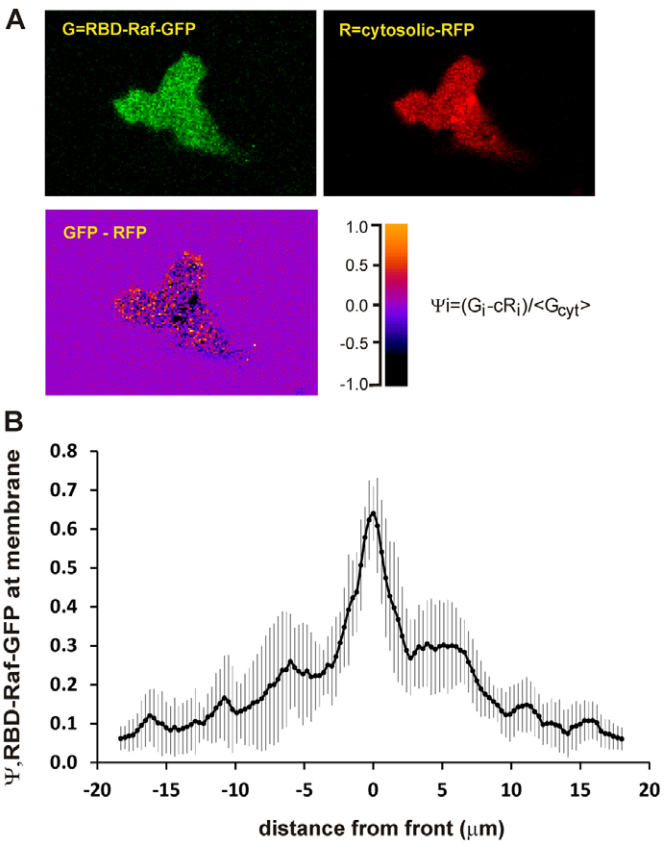

Fig. 1. Activated Ras-GTP in unstimulated cells. Wild-type cells in buffer expressing RBD-Raf–GFP and cytosolic RFP. (A) Images of a representative cell [GFP, RFP, GFP–RFP (Ψ)]. (B) Ras activation at the boundary (Ψ); data are the means±s.d. of 14 cells for different distances from the front of the extending pseudopod.

Multiple phases of Ras activation in cAMP gradients

The next question we wanted to answer was how the cAMP gradients influence the local accumulation of activated Ras. Wild-type cells expressing RBD-Raf–GFP and RFP were stimulated with a micropipette releasing cAMP (Fig. 2). The actual cAMP concentration around the cells was determined in control experiments using the fluorescent dye Alexa in the pipette. The cAMP concentration rapidly increases; at a distance of 50 μm from the pipette cAMP reaches half-maximal levels at ~3.2 s. At 60 μm from the pipette the cAMP concentration is not

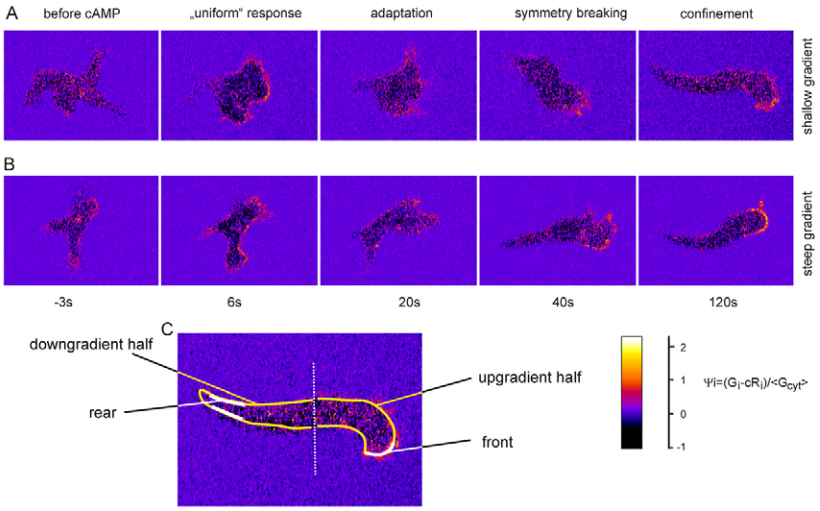

Fig. 2. Ras activation in cells stimulated with cAMP. Cells expressing RBD-Raf–GFP and cytosolic RFP were exposed to (A) a shallow cAMP gradient (28 pM/μm at 2.5 nM midpoint cAMP), and (B) a steep cAMP gradient (5000 pM/μm at 150 nM midpoint cAMP). Presented are images of typical cells at different times after exposure of the cells to these stimuli and the calculated Ψ of RBD-Raf–GFP at the membrane (Ψ). See supplementary material Movies 1 and 2 for the original experiment. (C) A schematic of the measurements in the cytoplasm and selected areas of the boundary.

only lower, but also half-maximal levels are reached about 1 second later. Thus a cell at this position receives at the upgradient side of the cell stronger and faster cAMP signals than at the down-gradient side. The measured cAMP concentration was used to calculate the local occupancy of the cAMP receptors with the known affinity of the receptor (Postma and van Haastert, 2009).

All cells exposed to a steep cAMP gradient (5000 pM/μm at a mean cAMP concentration of 150 nM) exhibit a strong and synchronous response (Fig. 2; supplementary material Movie 2), which allows detailed kinetic analysis of the translocation of RBD-Raf–GFP from the cytoplasm to the membrane (Fig. 3). Upon application of the cAMP gradient, RBD-Raf–GFP rapidly depletes from the cytoplasm, followed by a return to the cytoplasm around 15 seconds (Fig. 3A). In uniform cAMP, RBD-Raf–GFP remains in the cytoplasm, but in a cAMP gradient RBD-Raf–GFP returns to the membrane but only at the upgradient side of the cell (Fig. 2; Fig. 3B). This shows that Ras activation in cAMP gradients has three phases, which we first will describe for cells exposed to a steep cAMP gradient, inducing strong chemotaxis, and subsequently analyze in cells exposed to different cAMP gradients.

Initial ‘uniform’ response – excitation and adaptation of Ras activation

At about 6 seconds after application of a steep gradient of cAMP, RBD-Raf–GFP exhibits maximal translocation from the cytoplasm to the entire membrane in what appears a uniform response (Fig. 2; Fig. 3A). However, detailed measurement of the local levels of RBD-Raf–GFP at the membrane reveals a gradient of RBD-Raf–GFP at the membrane that is similar to the gradient of cAMP (Fig. 3E). Although these gradients are said to be steep for chemotaxis (20% concentration difference across the cell induces very strong chemotaxis), the differences in receptor occupancy between upgradient and downgradient sides of the cell are actually relatively small and the initial Ras activation exhibits a similarly small difference across the cell (Fig. 3E). After the initial translocation of RBD-Raf–GFP to the entire membrane, RBD-Raf–GFP starts to dissociate from the membrane. This dissociation is observed at the downgradient side of all cells; it occurs with a half-time of 4–6 seconds (Fig. 3B), is completed after ~30 seconds and never reoccurs in a stable cAMP gradient. In contrast, at the upgradient side of the cells, the dissociation of RBD-Raf–GFP from the membrane is followed by a return of RBD-Raf–GFP at the membrane (Fig. 3B). The response is more heterogeneous than at the downgradient side of the cell. In some cells dissociation of RBD-Raf–GFP from the membrane is nearly complete before it starts to return, whereas in other cells RBD-Raf–GFP starts to return at the membrane sooner, long before dissociation could be completed. The fraction of cells that exhibit late reappearance of RBD-Raf–GFP at the membrane was used to estimate the dissociation kinetics of RBD-Raf–GFP from the membrane at the upgradient side of the cell, and this appeared to be not statistically different from that at downgradient side of the cell (downgradient half-time, 5.8±1.1 seconds; upgradient half-time, 5.5±1.3 seconds, $n=4$ cells).

Symmetry breaking

As mentioned above, RBD-Raf–GFP starts to return to the membrane at the upgradient side of the cell at ~12 to 24 seconds after application of the pipette. Interestingly, when measured as the depletion of RBD-Raf–GFP from the cytoplasm, this recovery of RBD-Raf–GFP from cytoplasm to the membrane is completed after 30 seconds (Fig. 3B), but continues till 90 seconds when measured as the membrane level of RBD-Raf–GFP at the front of the cell (Fig. 3C), suggesting that activation of Ras at the leading edge is a complex process. Fig. 3D,F reveals that, at 30 seconds after stimulation, Ras activation occurs at a relatively large crescent of 15.6±1.4 μm, comprising ~40% of the circumference of the cell. At 90 seconds after stimulation, the crescent is much smaller (8.3±0.7 μm) with a concomitant increase of the intensity at the utmost leading edge of the cell. This suggests that gradient sensing comprises two processes: symmetry braking to induce Ras activation at the upgradient half of the cell, followed by confinement of activated Ras into a smaller crescent. Fig. 3C reveals that, in steep gradients, Ras activation in the upgradient half of the cell is ~10-fold larger than in the downgradient half of the cell. This symmetry breaking starts at ~16 seconds after application of the cAMP gradient, reaches half-maximal levels in ~6 seconds and is complete at 30 seconds after stimulation (Fig. 3G).

Confinement

The confinement of Ras activation into a smaller crescent in steep gradients is the slowest process. It starts at 20 seconds, has a half-time

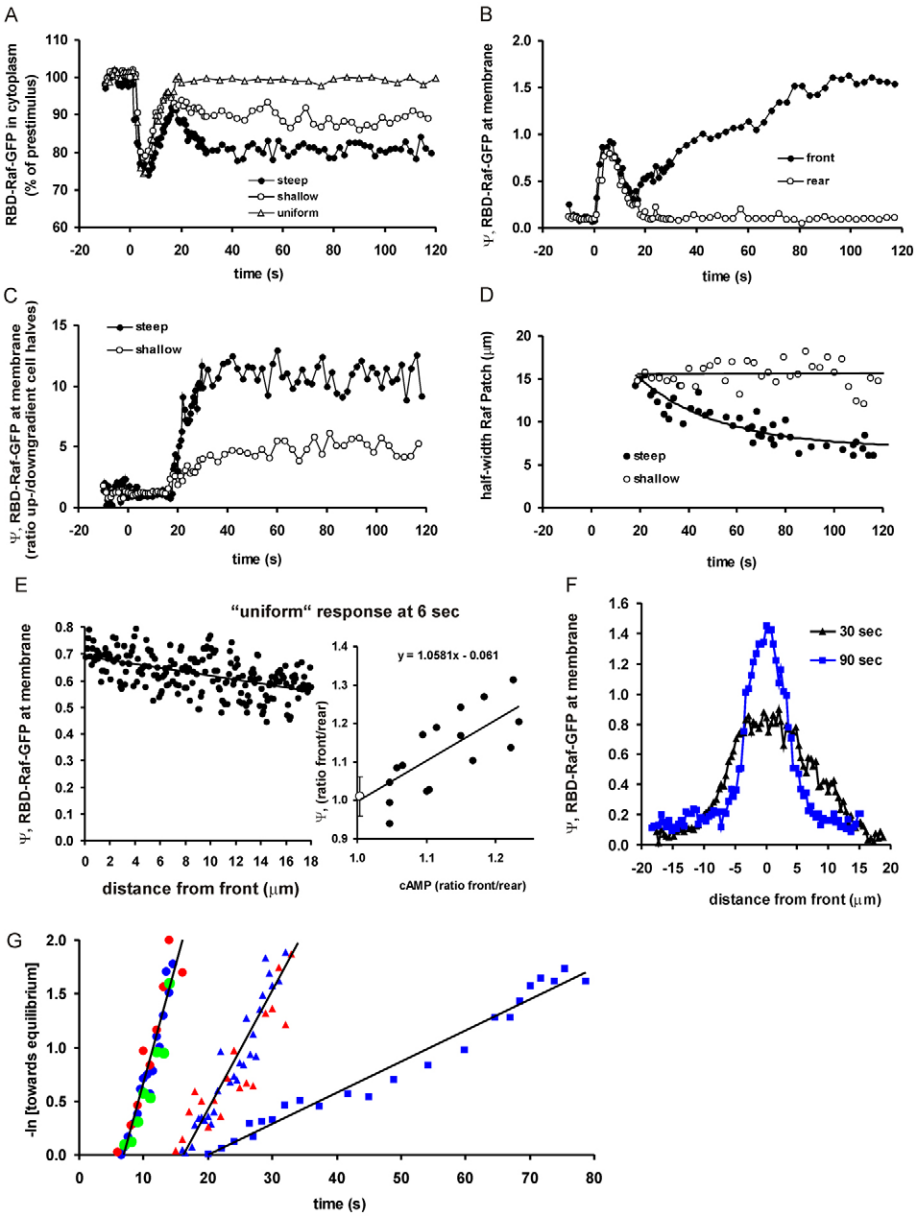

Fig. 3. Phases of Ras activation. Cells expressing RBD-Raf–GFP and cytosolic RFP were exposed to uniform cAMP (1 μM cAMP), a steep cAMP gradient or a shallow cAMP gradient as described in Fig. 2. (A) Kinetics of Ras-GTP activation presented as the depletion of RBD-Raf–GFP in the cytosol. (B) Kinetics of Ras-GTP activation in the membrane (Ψ) at the utmost front and the rear of the cell (defined as a small area at the side of the cell closest to and furthest away from the pipette, respectively) in a cAMP steep gradient. (C) Kinetics of Ras-GTP activation presented as the ratio of membrane bound RBD-Raf–GFP (Ψ) at the front half and rear half of the cell. (D) Kinetics of confinement of the activated Ras crescent. Measured was the width of the crescent at half-maximal height (see E). The data shown in panels A–D are the average of five cells. (E) The initial Ras activation at 6 seconds is directly proportional to the local activation of cAMP receptors. Left panel, Ras activation at different distances from the front at 6 seconds after application of a steep gradient; the data are from a typical experiment. Right panel, cells were exposed to cAMP gradients with different steepness and midpoint concentrations. We measured the local cAMP concentrations at the front and the rear of the cell using the dye Alexa; we also measured RBD-Raf–GFP at the boundary of the cell (Ψ). Each data point is a different cell, except the data at cAMP=1 (i.e. uniform cAMP), which is the mean±s.d. of five cells. The linear regression curve gives a slope of 1.06, indicating that the front and rear gradient of initial Ras activation is directly proportional to the front and rear gradient of receptor activation. (F) Ras activation at different distances from the front at 30 and 90 seconds after application of the steep gradient. (G) Kinetics of Ras-GTP activation after application of uniform (green), a shallow (red) or steep gradient (blue) of cAMP. Presented are logarithmic transformations of the data of panels A–D. The assumption is that adaptation, symmetry breaking and confinement are first order processes with rate constant k that start a specific time t_0, and thus follow the general equation $\ln(Y_t/Y_{final})=k(t-t_0)$, where Y is adaptation (decline of RBD-Raf–GFP at the membrane from A; $k=0.2$ s^{-1}, $t_0=7$ s), symmetry breaking (front-half:rear-half ratio from C; $k=0.1$ s^{-1}, $t_0=16$ s), or confinement (the width of the crescent from D; $k=0.03$ s^{-1}, $t_0=20$ s).

of 24 seconds and reaches a final level at about 2 minutes after stimulation (Fig. 3D,G). Between 30 and 90 seconds after stimulation, the crescent decreases in length by 50%, and this is accompanied by a ~2-fold increase of intensity of RBD-Raf–GFP at the leading edge of the cell (Fig. 3F). Thus, the notion of constant depletion levels of RBD-Raf–GFP in the cytoplasm while the

intensity at the leading edge increases (Fig. 3B,C) is caused by symmetry breaking to form a crescent of activated Ras and the confinement of activated Ras into a smaller crescent.

Gradient-dependent activation of Ras

Supplementary material Movie 3 shows the localization of RBD-Raf–GFP at the membrane before and after introduction of a micropipette producing a shallow cAMP gradient (28 pM/μm at a mean background concentration of 2.5 nM). Cells move towards the pipette with a chemotaxis index of 0.5 (i.e. with a small directional bias relative to the movement in buffer). The localization of RBD-Raf–GFP in these cells suggests a series of responses that is qualitatively similar to that in steep gradients, but smaller in magnitude. Fig. 2B presents typical images of RBD-Raf–GFP at the membrane in a shallow gradient. Upon application of a shallow cAMP gradient, RBD-Raf–GFP translocates from the cytoplasm to the boundary of the cell. As in steep gradients, translocation is maximal at ~6 seconds and recovers through adaptation. The kinetics of adaptation are nearly identical in shallow and steep gradients (half-time 7.6±1.7 seconds and 5.7±1.1 seconds in shallow and steep gradients, respectively; Fig. 3G). Following this activation and deactivation of Ras, RBD-Raf–GFP at the membrane starts to reappear at the upgradient half of the cell at a level that is about 5-fold to that at the downgradient half of the cell. This symmetry breaking in a shallow cAMP gradient follows the same kinetics as in a steep gradient and reaches a steady state at ~40 seconds after application of the gradient (Fig. 3C,G). The spatial activation of Ras is shown in Fig. 3D, revealing that RBD-Raf–GFP is localized at the membrane in a wide crescent. In contrast to a steep gradient, this large area of Ras activation does not confine with time to a smaller crescent with higher intensity. In summary, in a shallow cAMP gradient, initial activation and adaptation, as well as symmetry breaking are smaller but follow the same kinetics as in steep cAMP gradients. In contrast, confinement of Ras activation, and its induced polarization, does not occur in shallow cAMP gradients.

To determine the gradient-dependent activation of Ras, the experiments were repeated with pipettes containing different cAMP concentrations and cells were observed at different distances from the pipette. This provides a series of experimental conditions with gradients of different steepness of cAMP concentration. The chemotaxis indexes (CIs) of cells in these gradients are presented in Fig. 4D. To accommodate intrinsic Ras symmetry breaking, as well as gradient-induced symmetry breaking, we defined the front of the cell as the area from which a pseudopod is extended. In all these experiments, we observed no significant changes of RBD-Raf–GFP levels at the membrane in the rear half of the cell, which is ~10% of the level of RBD-Raf–GFP in the cytoplasm ($\Psi=0.10\pm0.01$).

In buffer, the front half of the cell contains ~3-fold more activated Ras compared with that in the rear half of the cell (Fig. 4A). cAMP gradients up to ~30 pM/μm induce only a slight increase of activated Ras in the front half of the cell compared with that of cells in buffer. Ras activation at the front of the cell increases with increasing steepness of the gradient, until the front half of the cell contains ~8-fold the amount of activated Ras than the rear half of the cell. Data are best fitted with a Hill plot that yields a Hill coefficient of $n=0.73$, and the gradient inducing half-maximal Ras activation ($K_{0.5}$) at the front was 220 pM/μm (Fig. 4A). Confinement of the crescent of

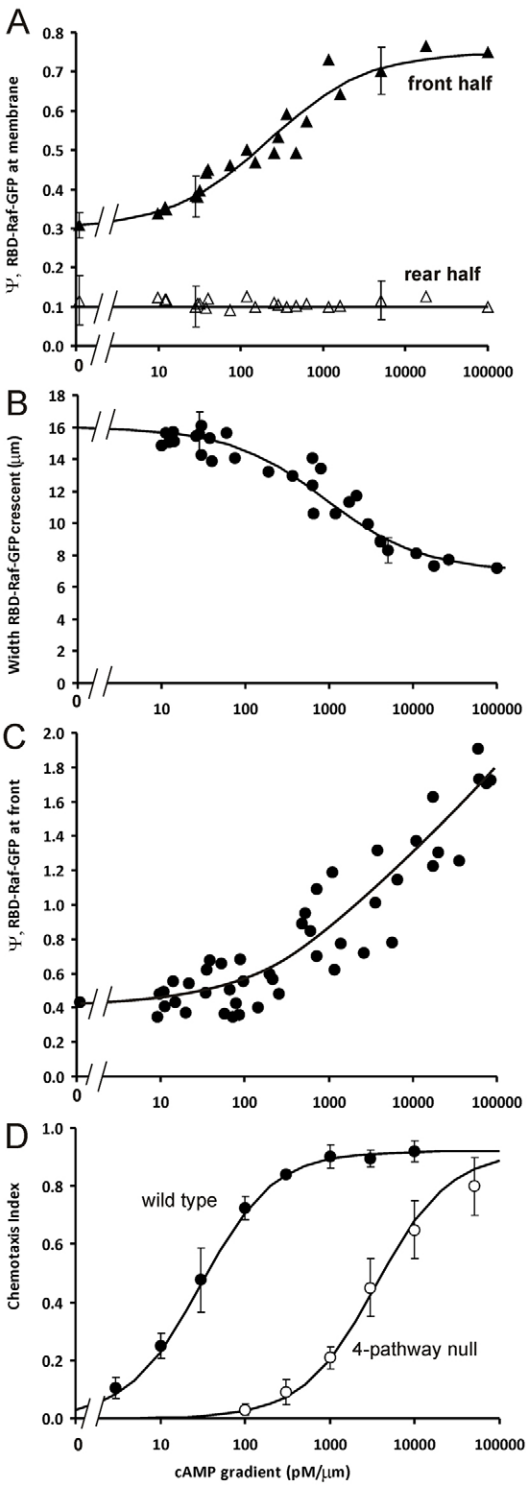

Fig. 4. Dose–response curves of Ras activation. Cells expressing RBD-Raf–GFP and cytosolic RFP were exposed to cAMP gradients with different steepness. The actual cAMP gradient was established using the dye Alexa that was mixed with cAMP. Ras-GTP activation along the cell boundary (Ψ) was measured as in Fig. 3F. These data were used to determine Ras activation in the front half and rear half of the cell (A), in the utmost front area of the cell (B), and the width of the activated Ras crescent at half-height (C). Data points with error bars are derived from the experiments presented in Fig. 3, and are the mean±s.d. of five cells; other data points are from single cells. (D) The chemotaxis index of cells in these gradients.

activated Ras upon longer exposure of cells to a cAMP gradient does not occur in shallow gradients below ~50 pM/μm (Fig. 4B). These data are also best fitted with a Hill plot that yields a Hill coefficient of $n=0.75$ and the $K_{0.5}$ for the crescent confinement was 890 pM/μm (Fig. 4B). The combination of symmetry breaking and confinement of the crescent in steep gradients leads to a ~5-fold increase of the intensity of RBD-Raf–GFP at the utmost front of the cell (Fig. 4C). Owing to the negative cooperativity (Hill coefficient <1) and the differences in $K_{0.5}$ for symmetry breaking and confinement of the crescent, this increase of Ras activation at the utmost front of the cell occurs over four orders of magnitude of cAMP gradient (Fig. 4C).

A predominant role for RasG in response to cAMP

Thus far, five *Dictyostelium* Ras proteins have been characterized in detail, and they all appear to have important and distinct roles in cell physiology; RasB is essential for cytokinesis, RasD regulates phototaxis and thermotaxis of multicellular slugs, RasS is important for the switch between eating and moving, and RasC and RasG together regulate all cAMP-mediated signaling in early development (Chubb et al., 2000; Chubb et al., 2002; Reymond et al., 1984; Sutherland et al., 2001; Weeks, 2005; Wilkins et al., 2000b). Although RasG is the predominant Ras protein detected by our marker, the RBD domain of mammalian Raf also binds with lower affinity to active RasC and probably all other *Dictyostelium* Ras proteins (Kae et al., 2004; Sasaki and Firtel, 2009). We here have used our sensitive assay to determine the specific contribution of RasC and RasG during the three cAMP-mediated activation phases. Cells with a deletion of *rasC* have only a slight defect in the uniform response and confinement, and show almost normal Ras activation at the leading edge of cells moving in a cAMP gradient (Fig. 5, Table 1). Several studies have shown that disruption of both *rasC* and *rasG* results in severe growth, developmental and chemotaxis defects (Bolourani et al., 2006; Kortholt et al., 2011). In contrast, a recent study showed that *rasC/rasG* double-null cells can undertake chemotaxis in response to both folate and cAMP (Srinivasan et al., 2013). Given that the cause of these conflicting data are unknown, but might be due to compensation by other pathways or upregulation of other Ras proteins, we instead used cells expressing dominant-negative RasGS17N from a tightly controlled doxycycline-inducible promoter (Veltman et al., 2009b). Wild-type cells expressing RasGS17N have reduced chemotaxis (CI=0.65±0,07) compared with that of wild-type cells (CI=0.88±0.10), exhibit a more than 50% reduction in the uniform response, show strong defects in symmetry breaking, and have no confinement. (Fig. 5, Table 1). Furthermore, *rasC*-null cells expressing RasGS17N have strongly impaired chemotaxis (CI=0.22±0.14), do not show a significant change in the localization of RBD-Raf–GFP, neither to uniform cAMP nor in a cAMP gradient (Fig. 5, Table 1; supplementary material Movie 4). Taken together, these results confirm previous genetic studies (Bolourani et al., 2006), and show that RasG is the key Ras protein in the regulation of cAMP mediated chemotaxis. However, *rasC*-null cells expressing RasGS17N show a strongly reduced, but significant, RBD-Raf–GFP translocation in response to uniform folate (supplementary material Table S2), suggesting that also other Ras proteins contribute to folate chemotaxis.

Different roles of G-protein subunits

The cAMP receptor activates the heterotrimeric G-protein Gα2βγ (Jin et al., 2000; Xiao et al., 1997). Mutant cells with a deletion of the single *gβ* gene do not show any changes in the localization of RBD-Raf–GFP, neither to uniform cAMP nor to a cAMP gradient (Fig. 6A). Cells also do not exhibit chemotaxis, confirming that Gβγ is essential for chemotactic signal transduction (Sasaki et al., 2004; Wu et al., 1995). Surprisingly, cells with a deletion of *gα2* do show a very significant translocation of RBD-Raf–GFP to the cell boundary in response to uniform cAMP (Fig. 6A). Expression of RasGS17N in *gα2*-null cells completely inhibits this RBD-Raf–GFP response, indicating that the detected Ras activation in *gα2*-null cells is completely dependent on RasG (Table 1). The RBD-Raf–GFP response is less pronounced in *gα2*-null cells compared with that in wild-type cells, and requires ~10-fold higher cAMP concentrations (Fig. 6C). The rate of Ras activation is initially the same in *gα2*-null and wild-type cells (Fig. 6B). However, in *gα2*-null cells, Ras activation stops after 3.8±0.7 seconds, whereas in wild-type cells activation continues until 6.0±0.9 seconds after stimulation with uniform cAMP (means±s.d., $n=8$).

As mentioned above for wild-type cells, a cAMP gradient initially induces a ‘uniform’ transient translocation of RBD-Raf–GFP to the cell boundary, which is followed by Ras activation at the side of the cell facing the cAMP gradient (supplementary material Movie 1). Also in *gα2*-null cells, the cAMP gradient induces a short transient uniform Ras activation, but in contrast to wild-type cells, the specific upgradient response never occurs (Fig. 6A); in addition, *gα2*-null cells do not exhibit any directional movement towards cAMP.

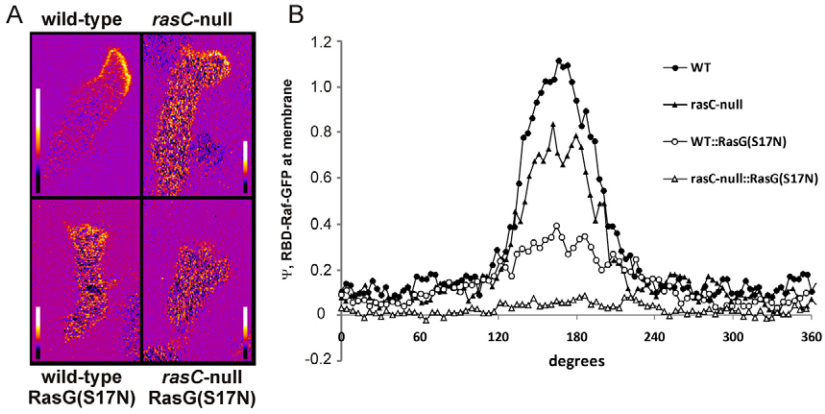

Fig. 5. Contribution of RasC and RasG. Wild-type and the indicated Ras mutants expressing RBD-Raf–GFP and cytosolic RFP were exposed to a steep cAMP gradient. Images of typical cells after exposure to these stimuli. (B) The calculated RBD-Raf–GFP at the membrane (Ψ). Ras activation along the cell boundary (Ψ) was measured as in Fig. 3F; data are the means of six cells and are presented as degrees from the extending pseudopod.

Table 1. Ras activation in mutants

	Initial 'uniform' response (% depletion in the cytoplasm)		Symmetry breaking (upgradient: downgradient ratio)		Width of crescent (μm)	
Cell	Mean	s.d.	Mean	s.d.	Mean	s.d.
WT	32.0	3.0	8.73	0.75	7.53	0.55
rasC-null	21.7*	8.4	4.39*	1.08	8.19	1.48
WT + RasGS17N	15.2*	5.4	2.13*	0.60	13.27*	0.67
rasC-null + RasGS17N	2.8*[a]	4.7	1.05*[c]	0.68	ND	
gβ-null	2.6*[a]	1.8	0.95*[c]	0.37	ND	
gα2-null	17.7*[b]	6.8	1.08*[c]	0.51	ND	
gα2-null + RasGS17N	1.2*[a]	5.6	ND		ND	
WT + LatA	31.0	6.6	12.71*	1.28	13.68*	1.68
4-p-null	33.0	4.6	6.86	1.73	12.42*	2.92
4-p-null +LatA	34.1	4.6	8.42	0.79	12.07*	0.32
gc-null	28.6	5.8	8.68	0.79	13.34*	0.99
myoII-null	33.0	5.2	7.72	1.99	12.47*	1.99
myo-null + LatA	35.7	2.3	8.12	1.41	12.57*	0.78
gefA-null	27.5*	3.6	4.03*	1.36	10.52	3.73
gefB-null	32.1	6.0	5.06*	1.21	8.76	1.78
gefC-null	28.2	2.9	2.97*	0.54	8.47	1.62
gefD-null	24.2*	2.6	2.96*	0.55	13.26*	2.07
gefE-null	38.1	5.6	3.90*	0.71	12.95*	1.90
gefG-null	35.5	2.8	2.56*	0.57	6.91	1.19
gefL-null	34.5	4.9	7.55	1.31	7.88	0.79
gefM-null	23.1*	7.6	2.98*	0.55	6.90	1.06
gefR-null	20.3*	4.7	2.22*	0.22	7.94	1.79
nfaA-null	31.4	5.5	3.40*	0.58	13.03*	1.98

Cells expressing both RBD-Raf–GFP and cytosolic RFP were exposed to a cAMP gradient (5000 pM/μm, mean concentration 150 nM). The initial 'uniform' response is the fluorescence intensity of RBD-Raf-GFP in the cytoplasm at ~6 seconds after application of the cAMP gradient. RBD-Raf-GFP at the cell boundary (Ψ) was calculated at 2 to 5 minutes after stimulation. Symmetry breaking is RBD-Raf-GFP at the cell boundary in the upgradient half of the cell divided by that in the downgradient half of the cell. The crescent of RBD-Raf-GFP at the cell boundary has a bell-shaped form. The width of the crescent at half-maximal height is presented. The data are the means and SD of eight wild-type or at least four mutant cells. WT, wild type; 4-p-null, cells with inhibition of four signaling pathways mediated by sGC, PLA2, PI3K and TorC2, were generated as previously described (Kortholt et al., 2011); ND, not determined because no crescent.

*$P<0.01$ compared with WT cells; [a], not significantly different from 0; [b], significantly different from 0; [c]not significantly different from 1.0.

Vegetative *Dictyostelium* cells respond to the chemoattractant folate, which activates many signaling pathways in a way that is similar to their activation by cAMP in starved cells. Folate chemotaxis requires activation of Gα4βγ (Hadwiger et al., 1994) and Ras at the leading edge (Lim et al., 2005). Whereas cells lacking gβ don't show any folate stimulated Ras activation, *gα4* (*gpaD*)-null cells still have a normal Ras response to uniform folate. As observed for cAMP in *gα2*-null cells, cells lacking *gα4*

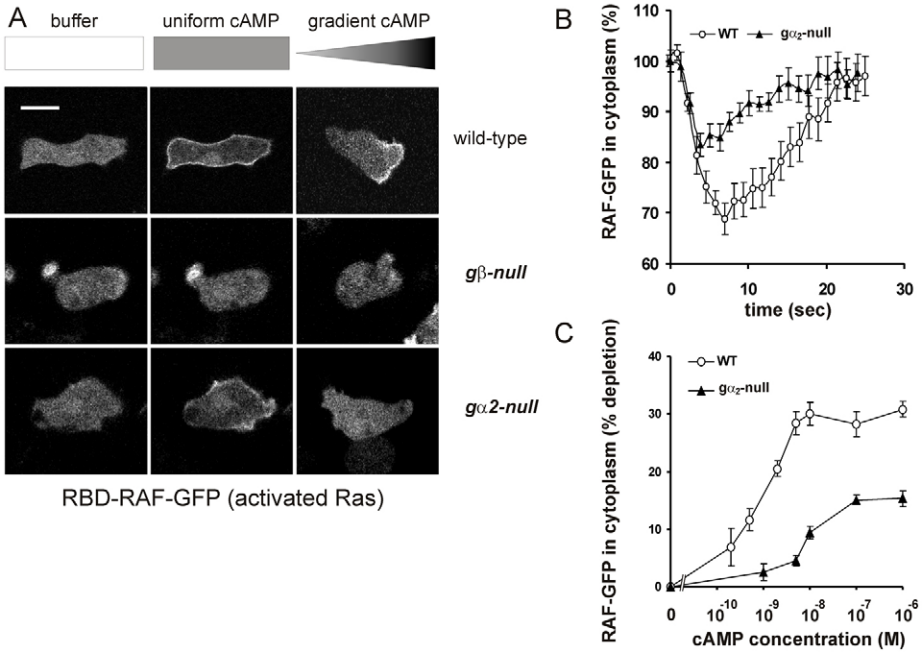

Fig. 6. Ras-GTP activation in *Dictyostelium* signaling mutants. (A) Representative images of RBD-Raf–GFP-expressing cells in buffer at 3–6 seconds after addition of uniform cAMP, or in a cAMP gradient. (B) The time course of translocation after uniform stimulation with 1 μM cAMP (means±s.e.m. of eight cells). (C) The response at 3–6 seconds after addition of uniform cAMP with different concentrations.

don't show the specific upgradient response or directional movement in a folate gradient (Kataria et al., 2013).

These results indicate different roles for Gβγ and Gα2 or Gα4 during chemotaxis. The experiments with wild-type, *gα2*-null and *gα4*-null cells suggest that Gβγ induces Ras activation, which is completely transient, even in a cAMP or folate gradient. Ras activation by uniform folate is about equal in wild-type and *gα4*-null cells, suggesting that Gα4 provides little contribution to Ras activation. However, a comparison of Ras activation by uniform cAMP between wild-type and *gα2*-null cells suggests that Gα2 contributes to Ras activation by which the response to uniform cAMP is prolonged. More importantly, in a cAMP or folate gradient, Gα2 or Gα4 mediates symmetry breaking by which Ras activation re-occurs at the side of the cell facing the chemoattractant, and cells move towards cAMP or folate.

Role of GEFs and GAPs

The genome of *Dictyostelium* contains 25 genes encoding for GEFs and 17 genes encoding for GAPs that potentially activate and inactivate Ras, respectively. Many of these genes have been inactivated by homologous recombination, without very severe effects on chemotaxis (Kortholt and van Haastert, 2008; Weeks, 2005; Wilkins et al., 2005). We have used our sensitive assay to measure Ras activation in nine mutants (Table 1). Recently, it has been shown that the GAP NfA regulates RasG activity during chemotaxis (Sasaki and Firtel, 2009); consistently *nfaA*-null cells show strongly reduced symmetry breaking and lack confinement (Table 1). The reduced symmetry breaking is the combined result of reduced Ras activation at the upgradient half and increased Ras activation at the downgradient half of the cell. All tested GEF mutants, with the exception of *gefL*-null cells, exhibit strongly reduced symmetry breaking, from ~8-fold in wild-type cells to only ~3-fold in the mutants. In all GEF mutants, this defect in symmetry breaking is caused by reduced Ras activation at the upgradient half of the cell. It should be noted that symmetry breaking is not absent in any mutant, suggesting that in wild-type cells symmetry breaking is mediated by multiple Ras GEFs.

The confinement of the crescent still occurs in mutants with a deletion of *gefB*, *gefC*, *gefG*, *gefL* and *gefM*, but is essentially absent in mutants lacking *gefD* and *gefE*. This suggests that a specific subset of GEFs and GAPs might be involved in restricting Ras activation to the utmost front of the cell. To investigate the role of confinement of Ras activation in a small crescent for cell shape, we have measured cell elongation defined as the ratio of the length to the width of the cell. The results (supplementary material Table S1; Fig. S2) indicate that there is no correlation between cell elongation and the Ras responses. For instance, *gefD*-null and *gefE*-null cells are both defective in confinement, but the *gefD*-null mutant is more elongated whereas *gefE*-null cells are far less elongated than wild-type cells.

The signaling pathways and cytoskeleton are important for confinement

Previously, it has been shown that the formation of F-actin, and the action of the four signaling enzymes PI3K, TorC2, PLA2 and sGC, are not required for Ras activation by uniform cAMP or in a cAMP gradient (Kortholt et al., 2011). These data were obtained for Ras localization at the leading edge in a stable cAMP gradient. Table 1 shows the data for the different phases of Ras activation upon application of the pipette releasing cAMP for wild-type, cells with a deletion or inhibition of all four signaling pathways, and *myosin*-null cells, all in the absence or presence of the F-actin inhibitor LatA. All cell lines exhibit a similar 'uniform' translocation of RBD-Raf–GFP to the membrane at ~6 seconds after application of the pipette, the subsequent dissociation of RBD-Raf–GFP from the membrane, and the reappearance of RBD-Raf–GFP at the leading edge. Symmetry breaking (the ratio of Ras activation in the upgradient half versus the downgradient half of the cell) is essentially identical in all these cell lines (Table 1). In contrast, the confinement of the crescent of activated Ras that occurs in wild-type cells exposed to steep gradients does not occur in cells with a deletion of the four signaling pathways, deletion of myosin II, or depletion of F-actin with LatA. Analysis of single pathway mutants show that cGMP is essential for confinement (the crescent is 13.3±1.0 μm in *gc*-null cells), whereas phosphatidylinositol (3,4,5)-triphosphate [PtdIns(3,4,5)P_3], TorC2 and PLA2 play a minor role in confinement (the crescent is 9.4±1.3 μm in wild-type cells in the presence of 50 μM PI3K inhibitor LY, 9.7±1.3 μm in *rip3*-null and *pkbR1*-null cells, and 7.9±2.1 μm in cells lacking *pla2*).

Discussion

With a sensitive assay to detect activated Ras at the plasma membrane, we showed here that *Dictyostelium* cells exhibit patches of activated Ras at the leading edge. Cells in buffer have about 3-fold more active Ras in the front half of the cell than in the rear half. This gradient of active Ras is also detectable in cells lacking *gβγ* or *gα2*, suggesting a mechanism of intrinsic symmetry breaking (Sasaki et al., 2007; supplementary material Fig. S1). An external gradient of chemoattractants further activates Ras. With the more sensitive assay to detect active Ras, we showed here that the chemotactic Ras activation consists of three phases. The first phase consists of activation and adaptation of the chemotactic machinery, and is essentially identical in uniform cAMP and in a cAMP gradient. Application of cAMP induces the translocation of RBD-Raf–GFP to the entire membrane and the formation of F-actin at the entire cortex. In both uniform cAMP and in a cAMP gradient, local Ras activation is proportional to the local activation of the receptor. Therefore, the initial Ras activation in a shallow gradient is only slightly stronger at the front than at the rear of the cell. The initial activation of Ras is transient; it is maximal after ~6 seconds and declines with a half-life of ~4–6 seconds owing to adaptation. This half-life is essentially identical in cells stimulated with uniform cAMP or with a shallow or steep cAMP gradient, and also identical at the front and the rear of the cell. Activation of Ras requires surface receptors and Gβγ, but surprisingly can occur in the absence of Gα2. In wild-type cells, most of the Gβγ is released by cAMP from Gα2βγ (Kumagai et al., 1989); in *gα2*-null cells Gβγ can be released from other cAMP-stimulated G-proteins, such as Gα1βγ and Gα9βγ (Bominaar and Van Haastert, 1994; Brzostowski et al., 2002). Activation of Ras in *gα2*-null cells is smaller in magnitude and requires higher cAMP concentrations than in wild-type cells. Three non-exclusive mechanisms might explain this reduced response: Gα2 contributes to Ras activation, as was suggested by the altered kinetics in *gα2*-null cells, less Gβγ is activated in *gα2*-null cells, or mixtures of wild-type and *gα2*-null cells do not develop completely normally. However, because cells lacking *gα4* show a similar Ras response to folate as *gα2*-null cells do to cAMP, the later mechanism seems to be unlikely.

The signaling enzymes PI3K, cGC, TorC2, and PLA2, as well as the cytoskeleton components F-actin and myosin have little effect on the initial activation and adaptation of Ras. In addition, deletion of the individual GEFs does not have a very strong effect on activation and adaptation, suggesting that multiple GEFs contribute to Ras activation. Importantly, at the end of this initial phase of Ras activation cells are in an adapted state.

After the initial transient activation, Ras becomes reactivated exclusively at the upgradient side of the cell. The magnitude of the response depends predominantly on the steepness of the gradient. Thus, in uniform 100 nM cAMP no reactivation of Ras is detectable, but strong activation of Ras is observed at the leading edge in a gradient of 10 nM/μm at a mean concentration of 100 nM cAMP. This symmetry breaking of Ras activation absolutely requires the presence of Gα2; in *gα2*-null cells a cAMP gradient induces the initial 'uniform' Ras response but not Ras activation at the leading edge and no chemotaxis. The signaling enzymes PI3K, sGC, TorC2 and PLA2 do not contribute to symmetry breaking of Ras activation in a cAMP gradient, neither does F-actin or myosin. The experiments suggest that symmetry breaking is mediated by Gα2. Since uniform cAMP induces stronger Ras activation in wild-type cells than in *gα2*-null cells, we propose that Gα2 contributes to Ras activation, presumably by activating additional GEFs or locally inhibiting GAPs. *Dictyostelium* contains 25 GEFs. Deletion experiments of nine GEFs reveal that in eight mutants symmetry breaking is strongly reduced, but not absent. These data suggests that multiple GEFs contribute to symmetry breaking.

During symmetry breaking, the downgradient half of the cell remains subject to adaptation, whereas Ras activation occurs in a relatively large crescent at the upgradient half of the cell. This crescent of membrane bound RBD-Raf–GFP has the highest intensity at the leading edge and gradually declines further away from the front as a bell-shaped curve with a width at half-height of ~15 μm. In wild-type cells, the crescent of activated Ras becomes more confined to the utmost leading edge, which is the third phase of Ras activation during chemotaxis. Confinement occurs without a change in the total amount of activated Ras, as indicated by the constant amount of RBD-Raf–GFP in the cytoplasm or at the entire boundary of the cell. The initial wide bell-shaped curve of membrane-bound RBD-Raf–GFP becomes very narrow, with very steep flanks. This suggests that during confinement of the crescent RBD-Raf–GFP dissociates from the ends of the crescent and binds to the utmost front. The local amount of active Ras-GTP depends on the local activity of GEFs and GAPs. The experiments suggest that during initial symmetry breaking, long-range gradients of GEFs at the front and GAPs at the rear lead to the large crescent of active Ras. During subsequent confinement a sharp spatial transition between active and inactive Ras is induced, suggesting that at the utmost front active Ras induces more GEF activity, whereas further away from the front GAPs are activated, leading to inactivation of Ras. Confinement of Ras activation to the leading edge requires F-actin and myosin, and the signaling molecules that regulate myosin, notably cGMP in *Dictyostelium*. An attractive model is that myosin filaments that accumulate at the side and rear of the cell during chemotaxis activate or recruit GAPs, whereas actin filaments that accumulate in the front activate or recruit GEFs. Confinement of Ras activation is normal in mutants with a deletion of *gefB*, *gefC*, *gefG*, *gefL*, *gefM* and *gefR*, but is absent in mutants lacking *gefD* and *gefE*, and *nfaA*. Interestingly, GefD contains a putative RhoGAP domain, suggesting a direct link with the actin cytoskeleton (Wilkins et al., 2005).

Expression of dominant negative RasGS17N in *rasC*-null cells results in a strongly reduced, but significant RBD-Raf–GFP translocation in response to uniform folate. This suggests that in addition to RasC and RasG, other Ras proteins contribute to folate signaling. By contrast, the current and previous experiments show that either RasC or RasG is necessary for the transduction of the cAMP signal and that RasG is the major Ras protein regulating cAMP-mediated symmetry breaking and confinement (Bolourani et al., 2006; Kortholt et al., 2011; Sasaki et al., 2004). Consistently, the strongest defects in symmetry breaking were observed for cells lacking *nfaA* and *gefR*, the only RasG-specific GAP and GEF, respectively, reported so far (Kae et al., 2004; Zhang et al., 2008). Much smaller defects in the chemotactic response were observed in cells lacking the RasC-specific *gefA* (Kae et al., 2007). However, the deletion experiments also show that activation, symmetry breaking and confinement use a multitude of Ras-GEFs, which are probably not all directly regulating RasG activity (Kae et al., 2007). Furthermore, during confinement the amplification pathways and cell cortex provide feedback regulation on Ras activity. This suggests that also other Ras proteins, activated downstream of RasG, can contribute to chemotaxis. Consistent with such a model, RapA is activated in a RasG-dependent manner, GefQ activates RasB in an actin-dependent manner, and both RasB and RapA are important for myosin II disassembly at the front of chemotaxing cells (Jeon et al., 2007; Mondal et al., 2008).

The combination of symmetry breaking and confinement leads to strong Ras activation at the leading edge. The ratio of active Ras at the front relative to the rear is ~10:1 in a steep gradient, where the ratio of receptor occupancy is only ~1.2:1, indicating that there is a strong spatial amplification of the cAMP signal. Interestingly, in shallow gradients (<30 pM/μm) very little amplification of the cAMP gradient is detectable at the level of Ras activation.

From movement in buffer to chemotaxis in shallow and steep gradients

In the absence of chemotactic signals, cells do not move in random directions, but exhibit a persistent random walk (Van Haastert and Bosgraaf, 2009). Cells have a high probability of extending a new pseudopod from the same Ras-activated area of the cell and in the same direction as the current pseudopod. This intrinsic pathway for symmetry breaking is independent of receptor or heterotrimeric G-protein signaling. At the lower limit of chemotaxis (~2 pM/μm), the very shallow gradient activates a few additional Ras molecules at the high-gradient side of the cell, which might induce a small gradient-oriented bias of the intrinsic Ras asymmetry thereby changing the probability of where actin polymerization occurs and a pseudopod is made. Somewhat steeper gradients (~100 pM/μm) induce more Ras-GTP molecules and therefore a stronger directional bias. Much steeper gradients (~2000 pM/μm) also induce amplification of Ras activation, providing full activation of Ras in the utmost leading edge of the cell. In these cells all pseudopods are formed in the direction of the steep gradient.

This cAMP gradient dose-dependent activation of Ras is similar in wild-type cells and in mutant cells lacking four

signaling enzymes (PI3K, TorC2, PLA2 and sGC) (Kortholt et al., 2011). Interestingly, these mutant cells can chemotax only in steep gradients with strong activation of Ras at the leading edge. Thus, the basal chemotaxis system, composed of cAMP receptors, Gα2βγ, RasC/G and Rac/actin, is sufficient for chemotaxis, but is relatively insensitive. The few molecules of Ras that are activated by the shallow gradient require the signaling enzymes PI3K, TorC2, PLA2 and sGC to induce a stronger directional bias. Previous experiments (Bosgraaf and Van Haastert, 2009) have shown that the signaling enzyme PLA2 and cGMP function in the memory of direction. Wild-type cells in buffer have the strong tendency to persist in their direction of movement, which is due to the alternating left–right extension of pseudopods at a small angle. The persistence of direction has a time constant of ~3 minutes, equivalent to ~10 pseudopods. In the absence of PLA2 and cGMP each new pseudopod is extended in a random direction. Thus, in wild-type cells, the small directional bias that is imposed by the shallow gradient slowly accumulates at each new pseudopod owing to the persistence memory of PLA2 and cGMP. The other signaling molecules and enzymes [PtdIns(3,4,5)P_3, TorCs and sGC] are formed at or localized to the place where Ras was activated. They enhance Ras-induced Rac activation and/or formation of F-actin at the leading edge. In the concept from physics, these signaling pathways enhance the signal-to-noise ratio, because they function as time-averaging and memory devices (PLA2 and cGMP), and as amplifier of spatial information [PtdIns(3,4,5)P_3, TorCs and sGC]. Taken together, these signaling pathways allow chemotaxis to occur in cAMP gradients that are ~100-fold more shallow (Fig. 4D).

Conclusions

These experiments provide a conceptual framework of gradient sensing and chemotaxis. A cAMP gradient induces the activation of the G-protein Gα2βγ. The Gβγ subunit induces the uniform activation and adaptation of Ras. The Gα2 subunit is essential to activate Ras at the side of the cell facing the highest concentration of cAMP. Local and global activities of specific GEFs and GAPs lead to Ras activation in a large area at the front of the cell. As cells start to move in the direction of the cAMP gradient, the rearranged cytoskeleton locally activates additional GEFs and GAPs to confine Ras activation to the utmost leading edge, thereby inducing polarized cells that move persistently towards cAMP. Downstream signaling molecules contribute to chemotaxis as memory of direction and amplifiers of spatial information.

Materials and Methods

Cell culture and preparation

The strains used are wild-type AX3, *rasC*-null (Bolourani et al., 2006), *gβ*-null (Wu et al., 1995), *gα2*-null (Kumagai et al., 1991), *gc*-null (Veltman and van Haastert, 2008), myoII-null (Yumura et al., 2005), *gefA*-null (Insall et al., 1996), *gefB*-null (Wilkins et al., 2000a), *gefC*-null, *gefD*-null, *gefE*-null, *gefG*-null, *gefL*-null (Wilkins et al., 2005), *gefM*-null (Arigoni et al., 2005), *gefR*-null (Kae et al., 2007) and *nfaA*-null (Zhang et al., 2008). RasG activation was inhibited by expressing dominant-negative RasGS17N from the previously described doxycycline-inducible vector pDM310 (Veltman et al., 2009b). Expression of RasGS17N from this dox-on system was induced by growing the cells for at least 24 hours in the presence of 10 μM doxycline. To determine the contribution of the signaling molecules, we used deletion mutants in specific genes in combination with drugs to inhibit one or a combination of sGC, PLA2, PI3K and TorC2 as previously described (Kortholt et al., 2011). Actin polymerization was inhibited with 5 μM Latrunculin A (LatA).

To study Ras activation, RBD-Raf–GFP (amino acids 50–134 of RAF1) was co-expressed with cytosolic mRFP from a modified pDM318 vector (Veltman et al., 2009a) in which the neomycin cassette was replaced by hygromycin. F-actin formation was visualized by expressing LimEΔcoil–GFP (amino acids 1–145 of LimE) from the previously published LB15B plasmid (Kortholt et al., 2011). Cells were grown in HL5-C medium including glucose (ForMedium) containing 50 μg/ml Hygromycin B (Invitrogen) for selection.

We have taken precautions to obtain mutant cells that exhibit optimal chemotaxis towards cAMP. Many *Dictyostelium* mutants with deletion of cAMP receptors, G-proteins or signaling enzymes do not acquire good chemotactic responsiveness to cAMP owing to impaired development and reduced expression of other signaling proteins. Development can be improved considerably by exogenous pulsing with cAMP or starving mutants in the presence of wild-type cells (Kortholt et al., 2011). Unlabeled wild-type cells were mixed with equal amounts of mutant cells expressing GFP- or RFP-tagged proteins, and starved on agar for 5 to 7 hours until streams were formed. Cells were then harvested, suspended in 10 mM KH_2PO_4/Na_2HPO_4, pH 6.5 (PB), and used in chemotaxis experiments.

Chemotaxis assays

To investigate how Ras is locally activated during chemotaxis, cells expressing RBD-Raf–GFP and RFP were stimulated with a micropipette releasing cAMP (Fig. 2). Cells were harvested in PB and incubated on a glass support at a density of ~4×10^4 cells/cm^2. The distance between adjacent cells is ~5 cell lengths, so that cells do not form streams, and chemotaxis can be measured in the absence of strong interactions between mutant and wild-type cells. Chemotaxis was observed using a confocal fluorescent microscope, detecting wild-type and mutant cells in the phase contrast and fluorescent channel, respectively. Control experiments using the fluorescent dye Alexa Fluor 594 in the pipette, and diffusion theory, reveal that at a distance of 50 μm from the pipette the spatial gradient is stable at 5 to 10 seconds after application of the pipette (Postma and van Haastert, 2009). Using pipettes with different cAMP concentrations and recordings at different distances from the pipette, cells are exposed to shallow or steep cAMP gradients (in pM/μm) at defined mean background cAMP concentrations (in nM). Confocal images were recorded using a Zeiss LSM 510 META-NLO confocal laser scanning microscope equipped with a Zeiss plan-apochromatic 63× NA 1.4 objective.

A sensitive assay for Ras activation at the cell boundary

In *Dictyostelium*, Ras proteins are present at the plasma membrane. Stimulation of cells with cAMP does not change the localization of Ras, but converts Ras from the inactive Ras-GDP state into active Ras-GTP. The RBD domain of mammalian Raf binds specifically to the GTP-form of Ras, mainly RasG. Upon cAMP stimulation, RBD-Raf–GFP translocates from the cytoplasm to the cell boundary (Fig. 2). The RBD-Raf–GFP response to cAMP is easy detectable, very reproducible and robust. However, assays measuring the activation of a membrane protein using the translocation of a cytosolic marker to the cell boundary are fundamentally insensitive. Assume a cell with no Ras activation and a fluorescence intensity of RBD-Raf–GFP in the cytosol equal to 100. The boundary pixels are on average half-filled with cytoplasm and have an intensity of 50. When a weak cAMP signal induces a small level of activation of Ras so that ~10% of cytosolic RBD-Raf–GFP translocates from the cytoplasm to the membrane, the intensity in the cytosol decreases to ~90, whereas the intensity in the boundary pixel increases to only 60–70%, which is still below the fluorescent intensity of the adjacent cytosolic pixel. Previously, we have demonstrated for a PtdIns(3,4,5)P_3 marker that such small translocations can be easily measured by co-expressing the GFP detector together with cytosolic RFP (Bosgraaf et al., 2008). Here, we co-expressed RBD-Raf–GFP and cytosolic RFP from one plasmid. The RBD-Raf–GFP minus the RFP signal in the boundary pixels represents Ψ, the amount of RBD-Raf–GFP that specifically binds to Ras-GTP at the membrane.

For calculations we used the following steps. First, the mean background fluorescence intensity in the red and green channels outside the cells is determined and subtracted from all pixels of the movie. Then individual cells are analyzed. To correct for the difference in expression levels of the two markers within one cell, large areas of the cytoplasm are selected (excluding nucleus and vacuoles), yielding the mean average fluorescent intensity in the cytoplasm of the red channel $<R_c>$ and green channel $<G_c>$, respectively. This provides the correction factor $c=<G_c>/<R_c>$, and all pixels in the red channel are multiplied by c. Then for each pixel (i) of that cell we calculated the difference of green and corrected red signal, and this is normalized by dividing by the average fluorescent intensity of GFP in the cytoplasm. Thus, $\Psi(i)=(G_i-cR_i)/<G_c>$. Previous analysis with a PtdIns(3,4,5)P_3 detector (Bosgraaf et al., 2008) and current analysis with the Ras-GTP detector (Fig. 2) reveal that this method provides a ~10-fold increase of sensitivity to detect local activated Ras. It should be noted that a value of $\Psi=0.4$ is highly significant and easily detectable using the information from the green and red channels, but is undetectable as an increase RBD-Raf–GFP at the cell boundary in the green channel only. Thus, all experiments yielding values of Ψ between 0 and ~0.5 yield new information on Ras activation not presented previously.

Acknowledgements

We want to thank Dr R. A. Firtel, Dr G. Weeks and the *Dictyostelium* stock center for providing the mutant strains used in this study.

Author contributions

A.K. and P.J.M.v.H. designed the experiments and wrote the paper. I.K.G. and R.K. performed the experiments.

Funding

This research received no specific grant from any funding agency in the public, commercial, or not-for-profit sectors.

Supplementary material available online at
http://jcs.biologists.org/lookup/suppl/doi:10.1242/jcs.132340/-/DC1

References

Ambrosi, D., Gamba, A. and Serini, G. (2004). Cell directional and chemotaxis in vascular morphogenesis. *Bull. Math. Biol.* **66**, 1851-1873.

Arigoni, M., Bracco, E., Lusche, D. F., Kae, H., Weeks, G. and Bozzaro, S. (2005). A novel Dictyostelium RasGEF required for chemotaxis and development. *BMC Cell Biol.* **6**, 43.

Bolourani, P., Spiegelman, G. B. and Weeks, G. (2006). Delineation of the roles played by RasG and RasC in cAMP-dependent signal transduction during the early development of Dictyostelium discoideum. *Mol. Biol. Cell* **17**, 4543-4550.

Bominaar, A. A. and Van Haastert, P. J. (1994). Phospholipase C in Dictyostelium discoideum. Identification of stimulatory and inhibitory surface receptors and G-proteins. *Biochem. J.* **297**, 189-193.

Bosgraaf, L. and Van Haastert, P. J. (2009). Navigation of chemotactic cells by parallel signaling to pseudopod persistence and orientation. *PLoS ONE* **4**, e6842.

Bosgraaf, L., Keizer-Gunnink, I. and Van Haastert, P. J. (2008). PI3-kinase signaling contributes to orientation in shallow gradients and enhances speed in steep chemoattractant gradients. *J. Cell Sci.* **121**, 3589-3597.

Bourne, H. R., Sanders, D. A. and McCormick, F. (1991). The GTPase superfamily: conserved structure and molecular mechanism. *Nature* **349**, 117-127.

Brzostowski, J. A., Johnson, C. and Kimmel, A. R. (2002). Galpha-mediated inhibition of developmental signal response. *Curr. Biol.* **12**, 1199-1208.

Causin, P. and Facchetti, G. (2009). Autocatalytic loop, amplification and diffusion: a mathematical and computational model of cell polarization in neural chemotaxis. *PLOS Comput. Biol.* **5**, e1000479.

Charest, P. G. and Firtel, R. A. (2007). Big roles for small GTPases in the control of directed cell movement. *Biochem. J.* **401**, 377-390.

Charest, P. G., Shen, Z., Lakoduk, A., Sasaki, A. T., Briggs, S. P. and Firtel, R. A. (2010). A Ras signaling complex controls the RasC-TORC2 pathway and directed cell migration. *Dev. Cell* **18**, 737-749.

Chen, L., Iijima, M., Tang, M., Landree, M. A., Huang, Y. E., Xiong, Y., Iglesias, P. A. and Devreotes, P. N. (2007). PLA2 and PI3K/PTEN pathways act in parallel to mediate chemotaxis. *Dev. Cell* **12**, 603-614.

Chubb, J. R., Wilkins, A., Thomas, G. M. and Insall, R. H. (2000). The Dictyostelium RasS protein is required for macropinocytosis, phagocytosis and the control of cell movement. *J. Cell Sci.* **113**, 709-719.

Chubb, J. R., Wilkins, A., Wessels, D. J., Soll, D. R. and Insall, R. H. (2002). Pseudopodium dynamics and rapid cell movement in Dictyostelium Ras pathway mutants. *Cell Motil. Cytoskeleton* **53**, 150-162.

Elzie, C. A., Colby, J., Sammons, M. A. and Janetopoulos, C. (2009). Dynamic localization of G proteins in Dictyostelium discoideum. *J. Cell Sci.* **122**, 2597-2603.

Hadwiger, J. A., Lee, S. and Firtel, R. A. (1994). The G alpha subunit G alpha 4 couples to pterin receptors and identifies a signaling pathway that is essential for multicellular development in Dictyostelium. *Proc. Natl. Acad. Sci. USA* **91**, 10566-10570.

Hoeller, O. and Kay, R. R. (2007). Chemotaxis in the absence of PIP3 gradients. *Curr. Biol.* **17**, 813-817.

Insall, R. H., Borleis, J. and Devreotes, P. N. (1996). The aimless RasGEF is required for processing of chemotactic signals through G-protein-coupled receptors in Dictyostelium. *Curr. Biol.* **6**, 719-729.

Jeon, T. J., Lee, D. J., Merlot, S., Weeks, G. and Firtel, R. A. (2007). Rap1 controls cell adhesion and cell motility through the regulation of myosin II. *J. Cell Biol.* **176**, 1021-1033.

Jin, T., Zhang, N., Long, Y., Parent, C. A. and Devreotes, P. N. (2000). Localization of the G protein betagamma complex in living cells during chemotaxis. *Science* **287**, 1034-1036.

Kae, H., Lim, C. J., Spiegelman, G. B. and Weeks, G. (2004). Chemoattractant-induced Ras activation during Dictyostelium aggregation. *EMBO Rep.* **5**, 602-606.

Kae, H., Kortholt, A., Rehmann, H., Insall, R. H., Van Haastert, P. J., Spiegelman, G. B. and Weeks, G. (2007). Cyclic AMP signalling in Dictyostelium: G-proteins activate separate Ras pathways using specific RasGEFs. *EMBO Rep.* **8**, 477-482.

Kamimura, Y., Xiong, Y., Iglesias, P. A., Hoeller, O., Bolourani, P. and Devreotes, P. N. (2008). PIP3-independent activation of TorC2 and PKB at the cell's leading edge mediates chemotaxis. *Curr. Biol.* **18**, 1034-1043.

Kataria, R., Xu, X., Fusetti, F., Keizer-Gunnink, I., Jin, T., van Haastert, P. J. and Kortholt, A. (2013). Dictyostelium Ric8 is a nonreceptor guanine exchange factor for heterotrimeric G proteins and is important for development and chemotaxis. *Proc. Natl. Acad. Sci. USA* **110**, 6424-6429.

Kortholt, A. and van Haastert, P. J. (2008). Highlighting the role of Ras and Rap during Dictyostelium chemotaxis. *Cell. Signal.* **20**, 1415-1422.

Kortholt, A., Kataria, R., Keizer-Gunnink, I., Van Egmond, W. N., Khanna, A. and Van Haastert, P. J. (2011). Dictyostelium chemotaxis: essential Ras activation and accessory signalling pathways for amplification. *EMBO Rep.* **12**, 1273-1279.

Kumagai, A., Pupillo, M., Gundersen, R., Miake-Lye, R., Devreotes, P. N. and Firtel, R. A. (1989). Regulation and function of G alpha protein subunits in Dictyostelium. *Cell* **57**, 265-275.

Kumagai, A., Hadwiger, J. A., Pupillo, M. and Firtel, R. A. (1991). Molecular genetic analysis of two G alpha protein subunits in Dictyostelium. *J. Biol. Chem.* **266**, 1220-1228.

Liao, X. H., Buggey, J. and Kimmel, A. R. (2010). Chemotactic activation of Dictyostelium AGC-family kinases AKT and PKBR1 requires separate but coordinated functions of PDK1 and TORC2. *J. Cell Sci.* **123**, 983-992.

Lim, C. J., Spiegelman, G. B. and Weeks, G. (2001). RasC is required for optimal activation of adenylyl cyclase and Akt/PKB during aggregation. *EMBO J.* **20**, 4490-4499.

Lim, C. J., Zawadzki, K. A., Khosla, M., Secko, D. M., Spiegelman, G. B. and Weeks, G. (2005). Loss of the Dictyostelium RasC protein alters vegetative cell size, motility and endocytosis. *Exp. Cell Res.* **306**, 47-55.

Mato, J. M., Losada, A., Nanjundiah, V. and Konijn, T. M. (1975). Signal input for a chemotactic response in the cellular slime mold Dictyostelium discoideum. *Proc. Natl. Acad. Sci. USA* **72**, 4991-4993.

Mondal, S., Bakthavatsalam, D., Steimle, P., Gassen, B., Rivero, F. and Noegel, A. A. (2008). Linking Ras to myosin function: RasGEF Q, a Dictyostelium exchange factor for RasB, affects myosin II functions. *J. Cell Biol.* **181**, 747-760.

Postma, M. and van Haastert, P. J. (2009). Mathematics of experimentally generated chemoattractant gradients. *Methods Mol. Biol.* **571**, 473-488.

Reymond, C. D., Gomer, R. H., Mehdy, M. C. and Firtel, R. A. (1984). Developmental regulation of a Dictyostelium gene encoding a protein homologous to mammalian ras protein. *Cell* **39**, 141-148.

Rivero, F. and Somesh, B. P. (2002). Signal transduction pathways regulated by Rho GTPases in Dictyostelium. *J. Muscle Res. Cell Motil.* **23**, 737-749.

Sasaki, A. T. and Firtel, R. A. (2006). Regulation of chemotaxis by the orchestrated activation of Ras, PI3K, and TOR. *Eur. J. Cell Biol.* **85**, 873-895.

Sasaki, A. T. and Firtel, R. A. (2009). Spatiotemporal regulation of Ras-GTPases during chemotaxis. *Methods Mol. Biol.* **571**, 333-348.

Sasaki, A. T., Chun, C., Takeda, K. and Firtel, R. A. (2004). Localized Ras signaling at the leading edge regulates PI3K, cell polarity, and directional cell movement. *J. Cell Biol.* **167**, 505-518.

Sasaki, A. T., Janetopoulos, C., Lee, S., Charest, P. G., Takeda, K., Sundheimer, L. W., Meili, R., Devreotes, P. N. and Firtel, R. A. (2007). G protein-independent Ras/PI3K/F-actin circuit regulates basic cell motility. *J. Cell Biol.* **178**, 185-191.

Srinivasan, K., Wright, G. A., Hames, N., Housman, M., Roberts, A., Aufderheide, K. J. and Janetopoulos, C. (2013). Delineating the core regulatory elements crucial for directed cell migration by examining folic-acid-mediated responses. *J. Cell Sci.* **126**, 221-233.

Sutherland, B. W., Spiegelman, G. B. and Weeks, G. (2001). A Ras subfamily GTPase shows cell cycle-dependent nuclear localization. *EMBO Rep.* **2**, 1024-1028.

Swaney, K. F., Huang, C. H. and Devreotes, P. N. (2010). Eukaryotic chemotaxis: a network of signaling pathways controls motility, directional sensing, and polarity. *Annu. Rev. Biophys* **39**, 265-289.

Tranquillo, R. T., Lauffenburger, D. A. and Zigmond, S. H. (1988). A stochastic model for leukocyte random motility and chemotaxis based on receptor binding fluctuations. *J. Cell Biol.* **106**, 303-309.

Tuxworth, R. I., Cheetham, J. L., Machesky, L. M., Spiegelmann, G. B., Weeks, G. and Insall, R. H. (1997). Dictyostelium RasG is required for normal motility and cytokinesis, but not growth. *J. Cell Biol.* **138**, 605-614.

Ueda, M. and Shibata, T. (2007). Stochastic signal processing and transduction in chemotactic response of eukaryotic cells. *Biophys. J.* **93**, 11-20.

Van Haastert, P. J. and Bosgraaf, L. (2009). Food searching strategy of amoeboid cells by starvation induced run length extension. *PLoS ONE* **4**, e6814.

van Haastert, P. J. and Postma, M. (2007). Biased random walk by stochastic fluctuations of chemoattractant-receptor interactions at the lower limit of detection. *Biophys. J.* **93**, 1787-1796.

Veltman, D. M. and van Haastert, P. J. (2008). The role of cGMP and the rear of the cell in Dictyostelium chemotaxis and cell streaming. *J. Cell Sci.* **121**, 120-127.

Veltman, D. M., Keizer-Gunnik, I. and Van Haastert, P. J. (2008). Four key signaling pathways mediating chemotaxis in Dictyostelium discoideum. *J. Cell Biol.* **180**, 747-753.

Veltman, D. M., Akar, G., Bosgraaf, L. and Van Haastert, P. J. (2009a). A new set of small, extrachromosomal expression vectors for Dictyostelium discoideum. *Plasmid* **61**, 110-118.

Veltman, D. M., Keizer-Gunnink, I. and Haastert, P. J. (2009b). An extrachromosomal, inducible expression system for Dictyostelium discoideum. *Plasmid* **61**, 119-125.

Vetter, I. R. and Wittinghofer, A. (2001). The guanine nucleotide-binding switch in three dimensions. *Science* **294**, 1299-1304.

Weeks, G. (2005). The small GTPase superfamily. In *Dictyostelium Genomics* (ed. Wiliam F. Loomis and Adam Kuspa), pp. 173-210. Horizon Bioscience.

Wilkins, A., Chubb, J. R. and Insall, R. H. (2000a). A novel Dictyostelium RasGEF is required for normal endocytosis, cell motility and multicellular development. *Curr. Biol.* **10**, 1427-1437.

Wilkins, A., Khosla, M., Fraser, D. J., Spiegelman, G. B., Fisher, P. R., Weeks, G. and Insall, R. H. (2000b). Dictyostelium RasD is required for normal phototaxis, but not differentiation. *Genes Dev.* **14**, 1407-1413.

Wilkins, A., Szafranski, K., Fraser, D. J., Bakthavatsalam, D., Müller, R., Fisher, P. R., Glöckner, G., Eichinger, L., Noegel, A. A. and Insall, R. H. (2005). The Dictyostelium genome encodes numerous RasGEFs with multiple biological roles. *Genome Biol.* **6**, R68.

Wu, L. J., Valkema, R., Van Haastert, P. J. M. and Devreotes, P. N. (1995). The G protein beta subunit is essential for multiple responses to chemoattractants in Dictyostelium. *J. Cell Biol.* **129**, 1667-1675.

Xiao, Z., Zhang, N., Murphy, D. B. and Devreotes, P. N. (1997). Dynamic distribution of chemoattractant receptors in living cells during chemotaxis and persistent stimulation. *J. Cell Biol.* **139**, 365-374.

Yumura, S., Yoshida, M., Betapudi, V., Licate, L. S., Iwadate, Y., Nagasaki, A., Uyeda, T. Q. and Egelhoff, T. T. (2005). Multiple myosin II heavy chain kinases: roles in filament assembly control and proper cytokinesis in Dictyostelium. *Mol. Biol. Cell* **16**, 4256-4266.

Zhang, S., Charest, P. G. and Firtel, R. A. (2008). Spatiotemporal regulation of Ras activity provides directional sensing. *Curr. Biol.* **18**, 1587-1593.